CLM-R110

United Kingdom Atomic Energy Authority
RESEARCH GROUP
Report

A LARGE DIAMETER Q-MACHINE PLASMA SOURCE WITH A ROTATIONALLY SYMMETRIC TEMPERATURE PROFILE

J BURT
P E STOTT

Culham Laboratory
Abingdon Berkshire
1971
Available from H. M. Stationery Office
C.18
PRICE 15p

UDC
621.039.619 Q-MACHINE
533.9.07

A LARGE DIAMETER Q-MACHINE PLASMA SOURCE WITH A ROTATIONALLY SYMMETRIC TEMPERATURE PROFILE

by

J. BURT
P.E. STOTT

ABSTRACT

The design and construction of a large diameter Q-machine source for lithium and other alkali metal plasmas is described. In order to minimize plasma losses due to endplate temperature asymmetries the plate is uniformly heated by electron bombardment from a rotating cathode.

UKAEA Research Group,
Culham Laboratory,
Abingdon,
Berks.

July, 1971 (IMG)

SBN: 85311 001 8

CONTENTS

1. INTRODUCTION

In a Q-machine gradients of plasma density and endplate temperature produce electric fields transverse to the axial magnetic field[1]. This results in an $\underline{E} \times \underline{B}$ plasma drift. Radial density and temperature gradients cause a plasma rotation which changes the frequency of azimuthally propagating waves when observed in the laboratory frame of reference[2]. Additional instabilities of the Kelvin-Helmoltz type may be generated if the rotation is strongly sheared[3]. Azimuthal asymmetries of density and temperature lead to radial drifts and enhanced cross-field plasma losses[4]. Consequently the plasma is not in complete thermodynamic equilibrium with the endplates[5] and the density will be less than that calculated by the well known theory for an equilibrium plasma[6].

In the STAMP experiment we are studying the magnetic shear stabilization of drift waves[7]. In looking for a correlation between the drift waves and radial plasma losses we must minimize the additional losses due to endplate asymmetries[8]. A further complication stems from the characteristic trefoil shaped magnetic surfaces produced by the stellarator-type helical windings. In order to avoid complex $\underline{E} \times \underline{B}$ drifts it is important to match the plasma equipotentials to the magnetic surfaces. The simplest practical way of achieving this is to ensure that the plate temperature is uniform and that the density profile is trefoil shaped.

An expression for the azimuthal electric field E_θ in terms of density n and plate temperature T is readily obtained[4,9] from Richardson's equation:

$$E_\theta = -\frac{kT}{er}\left\{\frac{1}{n}\frac{dn}{d\theta} - \left[\ell n\, n + \ell n\left(\frac{e}{A}\left(\frac{k}{2\pi m_e}\right)^{\frac{1}{2}}\right) - \frac{3}{2}\left(1 + \ell n\, T\right)\right]\frac{1}{T}\frac{dT}{d\theta}\right\}. \quad \ldots (1)$$

Here A is Richardson's constant (~ 100 A cm^{-2}sec^{-1} deg^{-2}), k is Boltzmann's constant, e and m_e are the electronic charge and mass. The quantity in square brackets in equation (1) which will subsequently be denoted by C is of the order of 25 and varies slowly with n and T. The electric field is thus much more sensitive to asymmetries in T than in n and the density dependence will be neglected.

The radial plasma flux per unit area $j_\perp = n v_\perp = n E_\theta / B$ where n is the plasma density and B the magnetic field. The total radial loss $J_\perp$ from a cylindrical plasma of length L and radius R is obtained by integrating $j_\perp$ over the surface of the column:

$$J_\perp = R L \int_0^{2\pi} j_\perp \, d\theta = \frac{k}{eB} L C \int_0^{2\pi} n \frac{dT}{d\theta} \, d\theta . \quad \ldots (2)$$

It is difficult to evaluate this integral exactly close to the edge of the plasma but approximately $J_\perp/n = L \frac{kT}{eB} C \frac{T_1}{T}$ where T is the mean plate temperature and T_1 is the difference between opposite edges. In Fig.1 $J_\perp/n$ is plotted against T_1 (for $T = 2500$ K, $L = 400$ cm and $R = 3.75$ cm). Other important loss mechanisms for a Q-machine are plotted in Figs.2, 3 and 4.

1.1 Drift Waves (Fig.2)

The radial flux density due to density and potential oscillations of the form $\tilde{n} = n_1 \cos m\theta$ and $\tilde{\varphi} = \varphi_1 \cos(m\theta - \delta)$ is given by:

$$j_r = \langle \tilde{n} \tilde{v}_r \rangle = \frac{1}{rB} \left\langle \tilde{n} \frac{d\tilde{\varphi}}{d\theta} \right\rangle = \frac{m}{2rB} n_1 \varphi_1 \sin\delta .$$

Note that for an outwardly directed flux δ is the phase angle by which $\tilde{n}$ leads $\tilde{\varphi}$. Approximating $m \sin\delta \sim 1$ and:

$$\frac{n_1}{n_o} \sim \frac{e\varphi_1}{kT} \quad \text{gives} \quad J_\perp/n \simeq L\left(\frac{kT}{eB}\right)\pi\left(\frac{n_1}{n_o}\right)^2 .$$

1.2 Collisional Diffusion (Fig.3)

$$J_\perp/n = 2\pi L D_{coll} = 2\pi L a_i^2/\tau_i$$

where a_i is the ion Larmor radius and τ_i is the ion collision time[10] including collisions with the endplates[11].

1.3 Endplate Recombination (Fig.4)

Ions striking the plates have a recombination probability:

$$\gamma = \left\{1 + \frac{g_i}{g_a} \exp\left[\left(\Phi_i - V_i\right)/T\right]\right\}^{-1} ,$$

where V_i is the ionization potential and Φ_i is the work function. The recombination is small ($\gamma \sim 10^{-3}$) for caesium and potassium, but relatively high ($\gamma \sim 0.5$) for sodium and lithium. The recombination is further reduced when the ions are trapped in the potential well between electron-rich sheaths at the endplates[5,6]. For a double-ended Q-machine the total recombination flux is given by:

$$J_R/n = \frac{\pi r^2}{4} n \, Ci \, Ce \, e^{V_i/kT} ,$$

where Ci and Ce are the ion and electron thermal velocities.

In low density plasmas when the ion mean free path is longer than the column length, the ions acquire sufficient directed energy on entering the plasma to penetrate the sheath at the opposite endplate[12]. In this case:

$$J_R/n = 4\pi r^2 \gamma Ci .$$

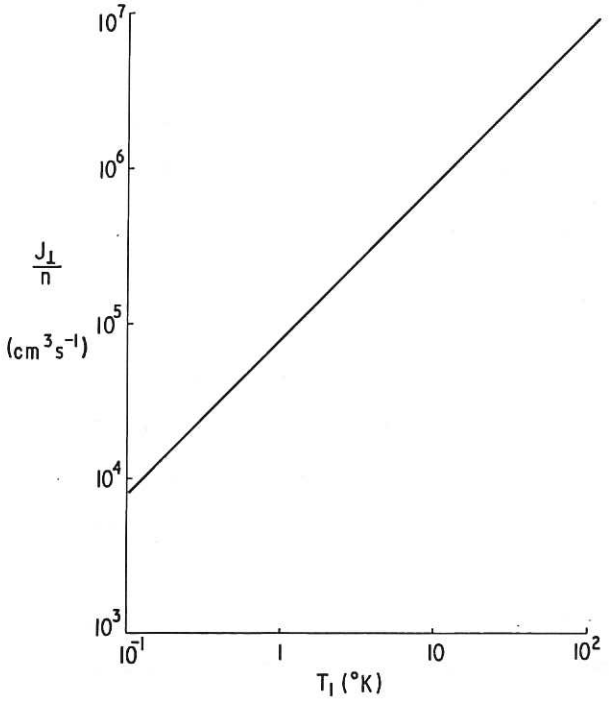

Fig.1 Radial particle losses due to temperature asymmetries. Estimated for a plasma column of central density n, length 400 cm, diameter 7.5 cm, and axial magnetic field 1000 G. T_l is the temperature difference across opposite edges of the end plate. Mean plate temperature is 2300 K.

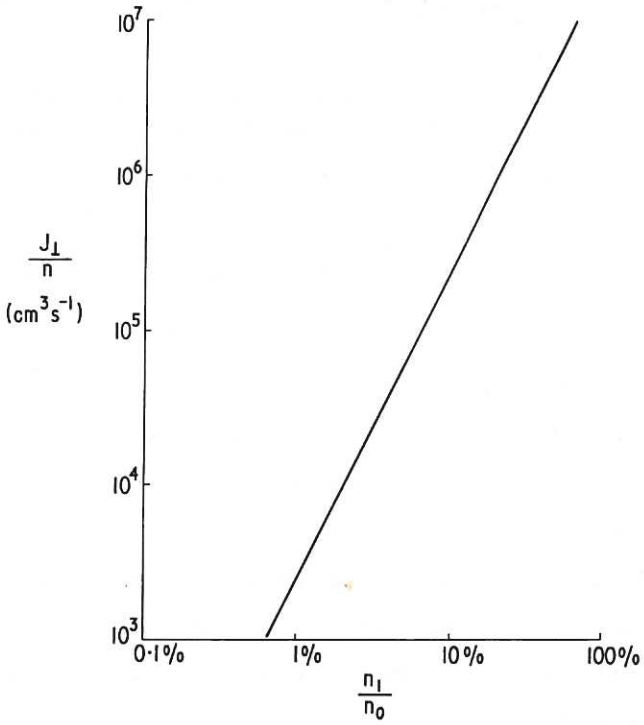

Fig.2 Radial particle losses due to drift waves. Estimated for a plasma column of central density n, length 400 cm, diameter 7.5 cm, and axial magnetic field 1000 G. n_l/n_o is the relative amplitude of the drift waves.

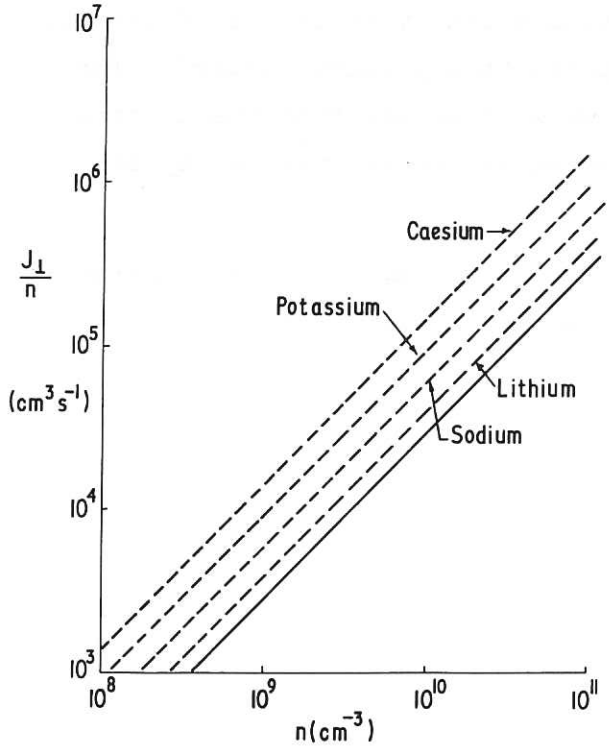

Fig.3 Radial particle losses due to collisional diffusion. Estimated for a plasma of central density n, length 400 cm, diameter 7.5 cm and field 1000 G. Full lines indicate losses due to electron-ion binary collisions and the broken lines include the additional losses due to ion collisions with the end-plates.

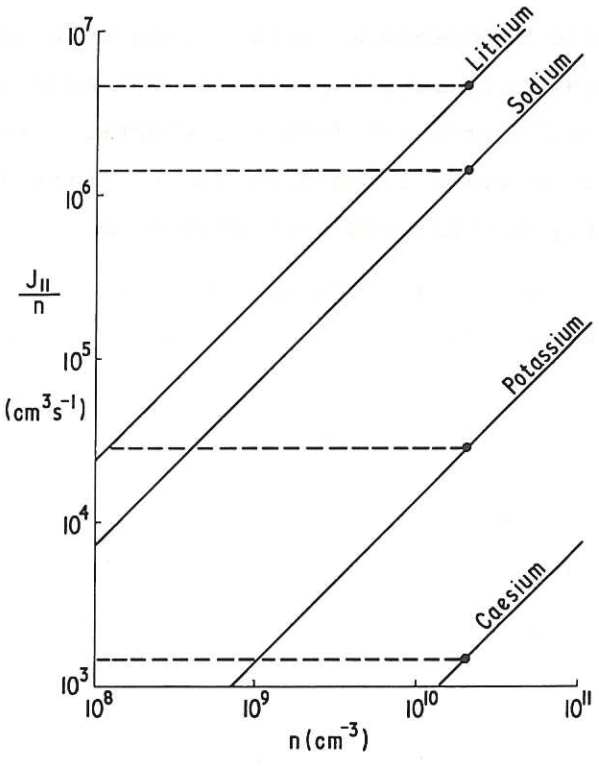

Fig.4 Recombination losses at the endplates. Estimates for rhenium discs 7.5 cm in diameter at 2500 K. The full lines denote the losses calculated for a plasma in thermodynamic equilibrium with $T_i = T_e = T_{plate}$. Broken lines are for collisionless plasma where the directed energy of ions gained from passing through the endplate sheaths is not thermalized by collisions. The large dots indicate the density at which the sheath potential is zero.

Comparing Figs.1 - 4, we can see two main effects due to temperature asymmetries:

(i) $J_\perp$ losses due to temperature asymmetries will be comparable to drift wave losses unless T_1 is very small (i.e. < 1 K).

(ii) The plasma density will also be substantially reduced unless T_1 is sufficiently small to make the $J_\perp$ losses smaller than the endplate recombination. This requires $T_1 < 50$ K for Li, 15 K for Na and 0.4 K for K.

Several methods for symmetrizing the endplate temperature were considered. We found that using a carefully designed filament and a double plate structure[9] we could produce a suitable radial temperature profile and obtain an azimuthal uniformity of about 10 K for a three inch diameter plate. In order to further improve the azimuthal temperature symmetry we decided to adopt the method suggested by Guilino[4] and rotate the filament behind the endplate. The alternative scheme of a rotating endplate and stationary filament was considered, but was found to be more difficult technically.

2. CALCULATION OF ROTATION SPEED

We will now estimate the improvement in temperature uniformity of a single homogeneous plate heated by a rotating slightly asymmetric filament. Radial temperature profiles have been computed in a previous paper[9] for several different filament shapes. Here we will assume that the temperature is radially uniform and that the filament may be represented by an evenly distributed heat source S.

Neglecting thermal conductivity of the plate supports, the temperature T at a radius r is given by the heat balance equation per unit plate area:

$$\Delta \rho s \frac{dT}{dt} = S - 2\alpha\sigma T^4 + \kappa\Delta\left(\frac{\partial^2 T}{\partial r^2} + \frac{1}{r^2}\frac{\partial^2 T}{\partial \theta^2}\right) \qquad \ldots (3)$$

Δ is the plate thickness, ρ the density, s the specific heat, κ the thermal conductivity, α the emissivity, and σ Stefans constant.

In the steady state the plate will attain a mean temperature:

$$T_o = \left(S_o/2\sigma\alpha\right)^{\frac{1}{4}}.$$

If the source is then suddenly shut-off

$$\Delta \rho s \frac{dT_o}{dt} = -2\alpha\sigma T_o^4 ,$$

i.e.

$$-\frac{1}{T_o}\frac{dT_o}{dt} = \tau^{-1} = \frac{2\alpha\sigma T_o^3}{\Delta \rho s} . \qquad \ldots (4)$$

Now consider a stationary sinusoidal azimuthal asymmetry of the source $S = S_o + S_1 \cos\theta \sin(\pi r/r_o)$ producing a corresponding temperature $T = T_o + T_1 \cos\theta \sin(\pi r/r_o)$ where $S_1/S_o \sim T_1/T_o \ll 1$. From equation (3):

$$T_1 = S_1 \left[8\,\alpha\sigma T_o^3 + K\Delta\left(\frac{1}{r^2} + \frac{\pi^2}{r_o^2}\right)\right]^{-1} . \qquad \ldots (5)$$

If the filament is now rotated at a constant angular frequency ω, the plate temperature variations will reach a new amplitude $T_1^* \ll T_o$ and will lag behind the filament by a phase angle δ.

$$S = S_o + S_1 \cos(\theta - \omega t) \sin(\pi r/r_o)$$

$$T = T_o + T_1^* \cos(\theta - \omega t + \delta) \sin(\pi r/r_o) .$$

Substituting in equation (3):

$$\omega \Delta \rho s\, T_1^* \sin(\theta - \omega t + \delta) = S_1 \cos(\theta - \omega t) - \left[8\,\alpha\sigma T_o^3 T_1^* + K\Delta\left(\frac{1}{r^2} + \frac{\pi^2}{r_o^2}\right)\right]\cos(\theta - \omega t + \delta) .$$

Collecting terms in $\sin(\theta - \omega t)$ gives:

$$\omega \Delta \rho s\, T_1^* \cos\delta = \left[8\,\alpha\sigma\, T_o^3\, T_1^* + K\Delta\left(\frac{1}{r^2} + \frac{\pi^2}{r_o^2}\right)\right] \sin\delta ,$$

i.e.

$$\tan\delta = \omega\tau \left[4 + K\tau\left(\frac{1}{r^2} + \frac{\pi^2}{r_o^2}\right) \Big| 4\rho s \right]^{-1} . \qquad \ldots (6)$$

Terms in $\cos(\theta - \omega t)$ gives:

$$T_1^*/T_1 = (1 + \tan^2\delta)^{-\frac{1}{2}} . \qquad \ldots (7)$$

The thermal time constant τ_o can be calculated from equation (4) or measured experimentally. For a 1 cm thick disc of rhenium the calculated value at $T_o = 2000$ K is about 60 secs which agrees with the value measured experimentally. The thermal conductivity term in the denominator of equation (6),

$$\frac{K\tau}{4\rho s}\left(\frac{1}{r^2} + \frac{\pi^2}{r_o^2}\right) \simeq 10 ,$$

and thus the thermal time constant can be cancelled out of equation (6) giving:

$$T_1^*/T_1 = \left[1 + f^2 x^2 \right]^{-\frac{1}{2}} \simeq 1/fx , \qquad \ldots (8)$$

where f is the rotation frequency (i.e. revolutions sec^{-1}) and

$$x = 2\pi\left[K\left(1 + \frac{\pi^2}{4}\right) \Big| r_o^2 \rho s \right]^{-1} \simeq 25$$

for a three inch diameter rhenium plate.

Thus as expected the plate temperature asymmetry is reduced as the rotation frequency is increased. The improvement expected from equation (8) is plotted in Fig.5. It can be seen from Fig.5 that a rotation speed of 25 r p m should reduce the temperature asymmetry by about one order of magnitude, whilst 250 r p m should give two orders improvement.

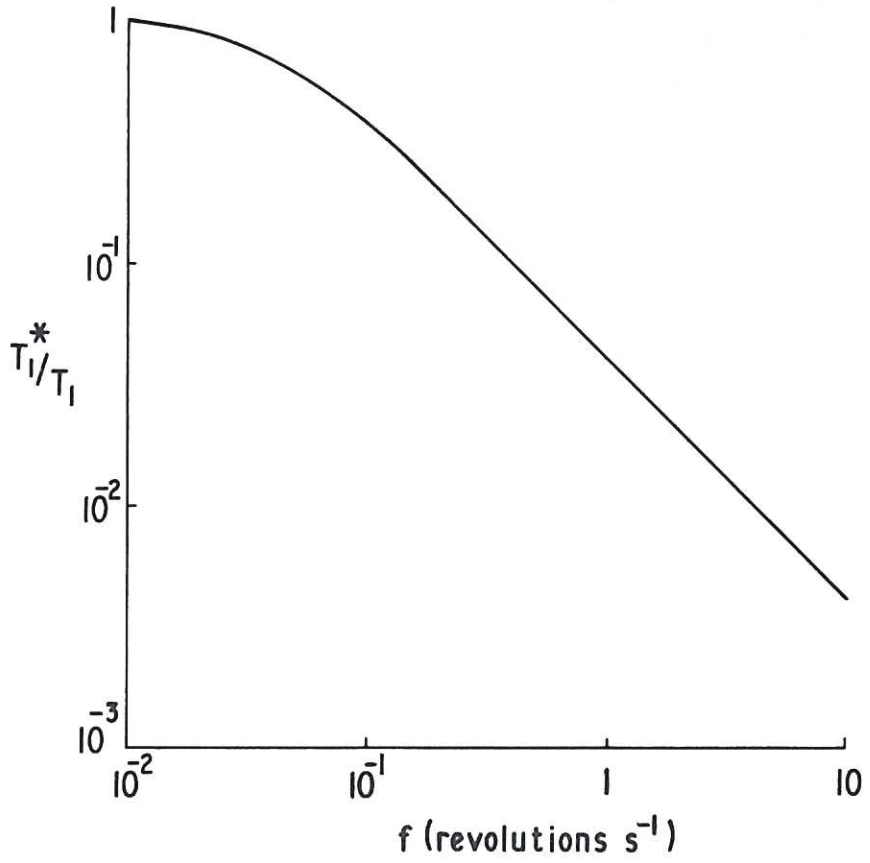

Fig.5 Calculated improvement of endplate temperature asymmetry T_1^* when the filament is rotated at a constant speed f compared to the asymmetry T_1 for a stationary filament.

3. DESIGN AND CONSTRUCTION OF THE SOURCE

The plasma sources for the STAMP experiment are designed to produce a column of plasma 7.5 cm in diameter and variable in length between 40 and 400 cm. Plasma is produced by thermal ionization of alkali metal vapour sprayed onto a rhenium plate which is maintained at a temperature of 2000 - 2500 K. The plate is heated by electron bombardment from the rotating filament placed 1 cm from the rear surface of the plate. The filament design has been described in a previous report[9].

A cut-away drawing of a complete plasma source is shown in Fig.6. To enable the plasma column length to be varied as previously stated, the source is mounted on the end of a polished stainless steel tube, 2¼" outside diameter, this tube enters the main vacuum vessel through a PTFE chevron type sliding vacuum seal which is differentially pumped. The overall length of the complete source is fifteen feet. Inside this polished tube a torque shaft is mounted in good fitting dry bearings at either end of the shaft and loose fitting bearings along the length of the shaft

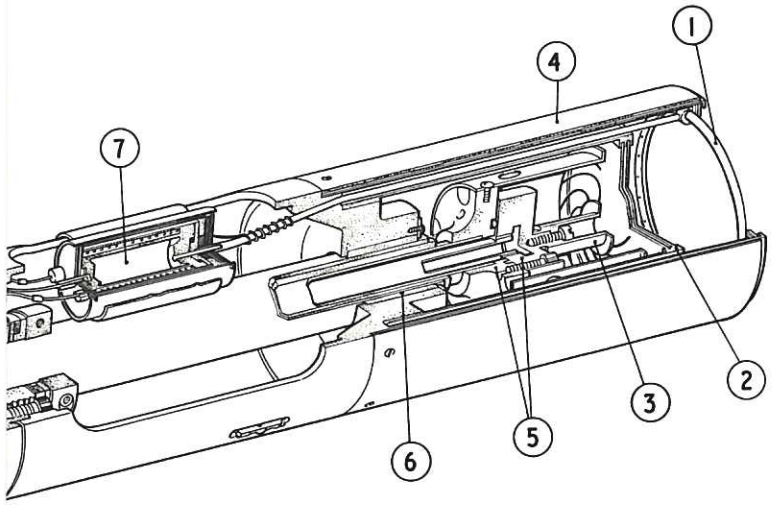

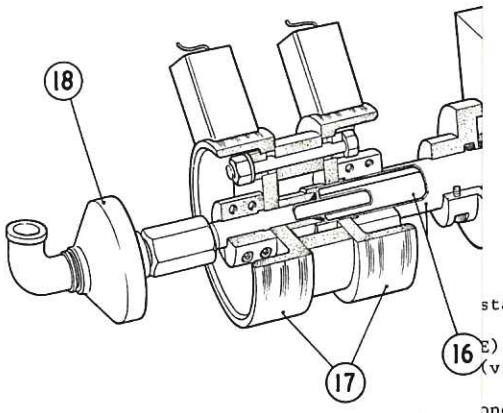

stainless
E)
(viton 'A'
onductors
d copper)
shed

(12) Sliding vacuum seal (PTFE and stainless steel)
(13) Bearing (filled PTFE)
(14) Rotary vacuum seal (viton 'A' rubber)
(15) Rotary water seal
(16) Water cooled conductors (copper)
(17) Slip rings (chrome-copper)
(18) Rotary water seal

support the weight. The shaft whips slightly in the central region during rotation. A rotating vacuum seal is also used at each end of the shaft and the volume between these two seals is pumped to a pressure of about 10^{-3} torr. The shaft is driven by a belt and pulley drive, mounted at the cold end at atmospheric pressure, whilst the filament at the hot end, operates in a high vacuum. The filament terminal blocks, the bearing and rotating vacuum seal housing at the hot end are water cooled, past experience having shown the importance of fixing temperature boundaries if long term temperature drifts are to be avoided.

3.1 The Rotating Shaft

The shaft was designed to perform the following duties:

(a) Insulate the filament from earth for 3 kV d.c. working.

(b) Carry 150 A d.c. filament heating current.

(c) Carry water for cooling filament terminal blocks.

(d) Provide surfaces for bearings and rotating vacuum seals.

(e) The shaft to be compatible with a high temperature and vacuum environment at one end.

(f) The complete shaft to be vacuum tight.

The shaft consists of three coaxial tubes, each about 14 feet long. The outer tube, on which the driving pulley is fitted, is at earth potential and is made of 304 type stainless steel, 1¼ inches o.d. x .060 inch wall thickness. At each end of this tube, twelve inches of the outer surface is polished to provide surfaces for bearings and rotating vacuum seals. Inside of this tube and separated by a radial gap of ⅛" is a ¾" nominal bore copper tube, which carries 150 A heating current to the filament and water for cooling the filament terminal blocks. A copper flange acts as a terminal block, and is brazed to the hot end of this tube. A copper alloy slip-ring and a rotating water seal are clamped to the cold end of the tube. The ⅛" radial gap separating these two outer tubes is filled with a silicone rubber I C I Silcaset 101. This rubber provides 5 kV electrical insulation, makes a good vacuum seal and transmits driving torque between the two tubes.

The inner most tube of this coaxial shaft assembly is a ⅜" o.d. copper tube held concentric in the ¾" bore copper tube by P T F E spacers which do not unduly impede the flow of cooling water. At the hot end of this tube a solid flange made of molybdenum is vacuum brazed. This acts as the second terminal block for the filament. Water channels machined in this flange ensure good water cooling which is carried by this tube in addition to the 150 A filament heating current. A slip ring and rotating water seal are also

clamped to this tube at the cold end. To provide some electrical and thermal insulation between the two current carrying tubes, a .005" thick Kynar sleeve is heat shrunk on to this innermost tube. Thermal insulation is necessary to prevent heat exchanger effects between the two tubes. The two flanges forming the filament terminals are bolted together at the hot end by molybdenum bolts which are insulated by boron nitride bushes. A silicone rubber 'O' ring between the flanges acts as a water and vacuum seal and provides electrical insulation between the filament terminals. A small potential drop of 3 volts exists between these terminals during operating. Torque is transmitted to the inner tube by bolting together the terminal flanges as stated at the hot end, and at the cold end by bolting the two slip rings together by PTFE insulated bolts.

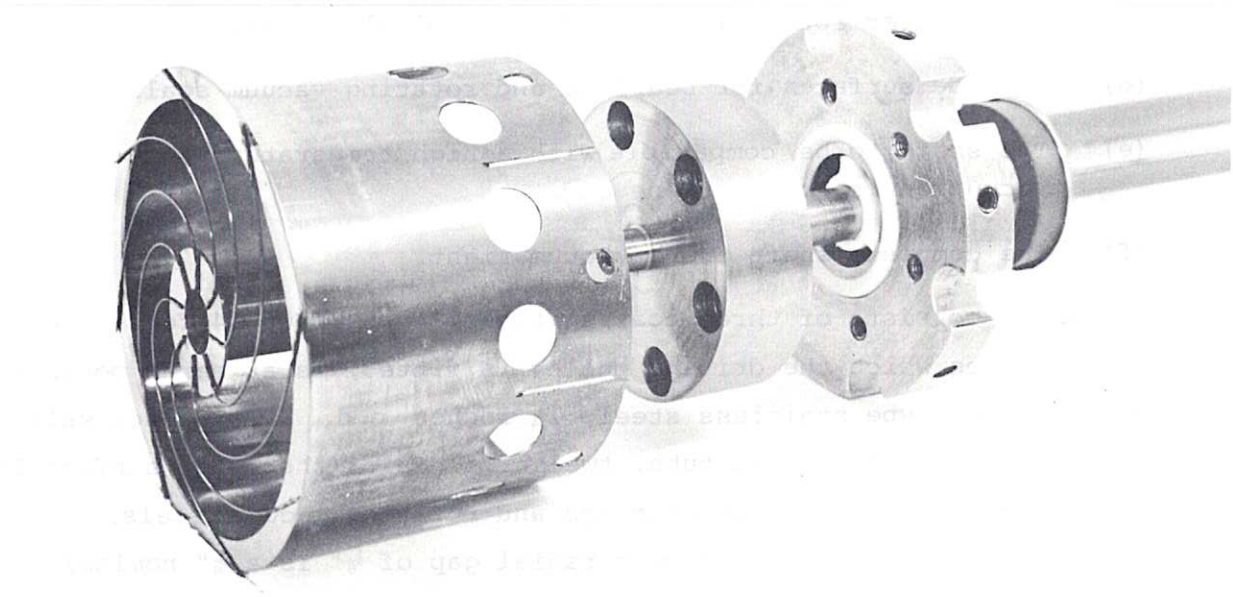

Fig.7 'Hot end' of the rotating torque shaft showing the water cooled filament blocks and coaxial tube assembly.

A view of the hot end of the shaft assembly is shown in Fig.7. Difficulties experienced during the manufacture and subsequent operation of the rotating shaft were mainly concerned with the insulation in the $\frac{1}{8}$" radial gap between the stainless steel and copper tubes. Epoxy resins were tried but were unsatisfactory from the vacuum point of view, due to poor adhesion to the metal surfaces and shrinkage during curing, which caused vacuum leaks along the length of the shaft. Silicone rubber has proved more satisfactory than the epoxy resins, although we have experienced a vacuum leak along the shaft length with this material. The silicone rubber is very viscous and takes about ninety minutes to be vacuum drawn the length of the tubes even whilst being pumped under pressure from the opposite end.

The small amount of catalyst used with the silicone rubber, 0.1 to 0.3%, to give a working life greater than the drawing time, must be carefully mixed before use. Care must also be taken with cleaning and priming the metal tubes, prior to filling with the rubber.

3.2 Shaft Bearings

As previously stated dry bearings are used in which to rotate the shaft. At the hot end two split sleeve bearings are fitted, the one nearer the hot plate and experiencing a high temperature is made of boron nitride whilst the other is graphite filled PTFE. This same material is also used for the bearing at the cold end of the shaft and is of similar design. The weight of the shaft is supported along its length by loose fitting PTFE supports spaced at eighteen inch intervals along the shaft length. No measurement of the wear rate of the bearings has been carried out but operation is still satisfactory after many hours running.

3.3 Rotating Vacuum Seals

A vacuum seal is fitted at each end of the rotating shaft and the volume in between is pumped by a mechanical pump. The seals currently in use are chevron type seals made of Viton 'A' rubber and speeds of up to 200 r p m (80 ft/min) have been achieved and continuously used. Speeds greater than 200 r p m have not been tried with this type of seal.

Using virgin PTFE chevrons for the seals, resulted in leaks at speeds below 100 r p m (40 ft/min); and their use was discontinued. A face type rotating vacuum seal, using a filled PTFE seal and a stainless steel bellows, has been designed but not yet tested. This new seal should produce far less hydrocarbon contamination than those in current use.

4. CONCLUSIONS

The hotplate temperature was measured by an optical pyrometer sensitive to the wavelength range 0.5 to 1.2 microns (Land type NQO 9/500/20 AE). The instrument was mounted outside the vacuum vessel behind a glass window and could be scanned across the hotplate by means of a 45° mirror attached to a moving probe. When operated at its focal distance of 50 cm, the pyrometer had a resolution of 0.15 cm. After amplification by 30 dB to millivolt level, the pyrometer output was displayed on a chart recorder. The readings were corrected for plate emissivity and transmission losses in the optical system and were converted to degrees using a black body source calibration chart. The sensitivity of the pyrometer at plate temperatures of 2000 K was of the order of 0.2 K, and the absolute accuracy was better than 100 K, this being limited by the value taken for the emissivity of rhenium.

Typical temperature profiles taken diametrically across the hotplate are shown in Fig.8. A marked improvement in the temperature symmetry can be seen when the filament is rotated. In Fig.9 the magnitude of the temperature asymmetry is plotted against the rotation speed, for measurements made over a range of mean plate temperatures. These results confirm that the temperature symmetry of a large diameter hotplate can be improved by some two orders of magnitude when the filament is rotated at speeds of up to 200 revolutions per minute.

The effect of the improved temperature symmetry on the containment of thermally generated plasmas will be discussed in more detail in a later report, but preliminary results indicate a marked improvement in plasma containment.

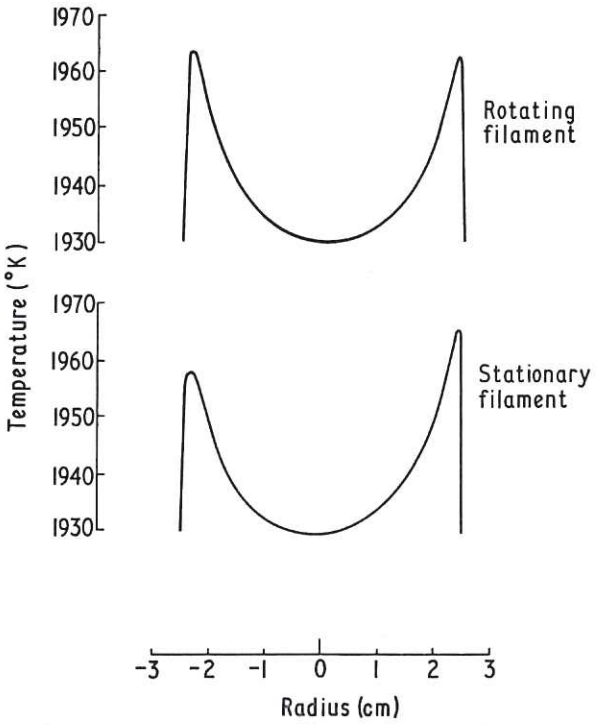

Fig.8 Hotplate temperature profiles.

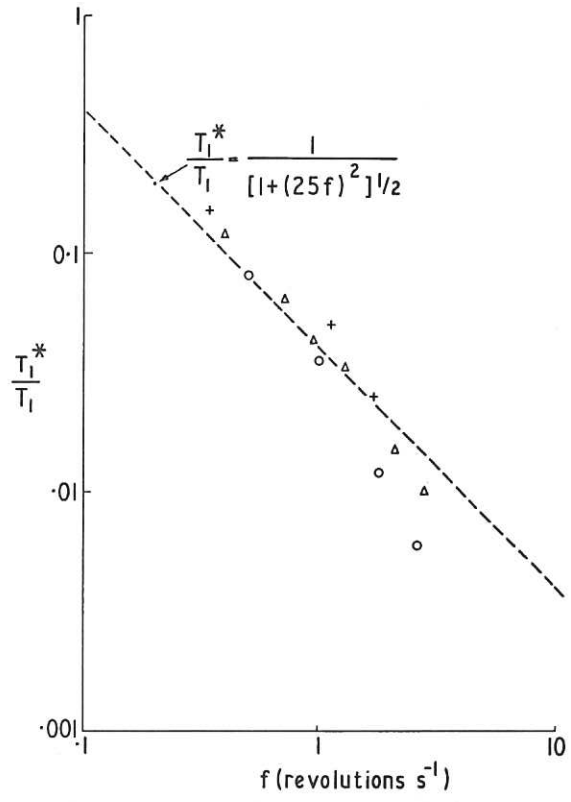

Fig.9 Measured improvement of endplate temperature T_1^* when the filament is rotated at constant speed f revolution per second compared to the asymmetry T_1 for a stationary filament.

+ Mean plate temperature T_o = 1850 K
Δ Mean plate temperature T_o = 2000 K
O Mean plate temperature T_o = 2170 K

ACKNOWLEDGEMENTS

It is a pleasure to acknowledge the valuable contributions to this work by K. Lavender and W. Smith during the design stages, and by R. Dyer, G. Gigg and I. Hammond during the construction and testing.

REFERENCES

1. CHEN, F.F. Plasma Physics Laboratory Report MATT 472 , Princeton University, (1966).

2. LITTLE, P.F. and MIDDLETON, C.R. Nucl. Fusion, 9, 67 (1969).

3. JASSBY, D.L. and PERKINS, F.W. Phys. Rev. Letters, 24, 256, (1970).

4. GUILINO, E. Phys. Fluids, 13, 1855, (1970).

5. GOELER, S. von and MOTLEY, R.W. Phys. Fluids, 13, 834, (1970).

6. GOELER, S. von, Phys. Fluids, 7, 463, (1964).

7. STOTT, P.E., BURT, J. and LITTLE, P.F., Phys. Rev. Letters, 25, 996, (1970).

8. MOSHER, D. and CHEN, F.F., Phys. Fluids, 13, 1328, (1970).

9. BURT, J., LITTLE, P.F. and STOTT, P.E. Culham Laboratory Report CLM - R 98 , (1969).

10. SPITZER, L. Jr., 'Physics of Fully Ionized Gases', Interscience, New York, (1962).

11. GREIGER, G., Report MPI-PA-15/64, Max-Plank Institut für Physik und Astrophysik, München, (1964).

12. HASHMI, M., HOUVEN van OORDT, A.J. van der, and WEGROWE, J., Nuclear Fusion, 10, 163, (1970).

Available from

HER MAJESTY'S STATIONERY OFFICE

49 High Holborn, London, W.C.1
13a Castle Street, Edinburgh 2
109 St. Mary Street, Cardiff CF1 1JW
Brazennose Street, Manchester M60 8AS
50 Fairfax Street, Bristol BS1 3DE
258 Broad Street, Birmingham 1
7-11 Linenhall Street, Belfast BT2 8AY

or through any bookseller.